Supplement of Biogeosciences, 23, 441–462, 2026
https://doi.org/10.5194/bg-23-441-2026-supplement

Biogeosciences Open Access EGU

Supplement of

Combined water table and temperature dynamics control CO_2 emission estimates from drained peatlands under rewetting and climate change scenarios

Tanja Denager et al.

Correspondence to: Tanja Denager (tad@geus.dk)

This supplementary material contains Figure S1–S9 and Table S1–S7, which provide additional data and visualizations in support of the main manuscript.

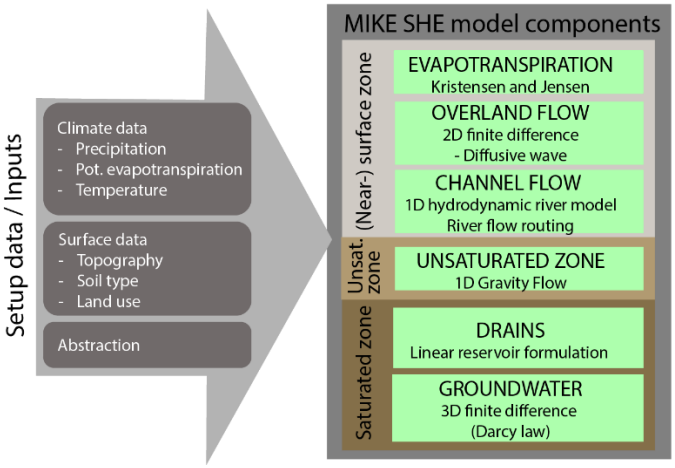

Figure S1: MIKE SHE model components used in the Tuse catchment model. Evapotranspiration model by Kristensen and Jensen (1975)

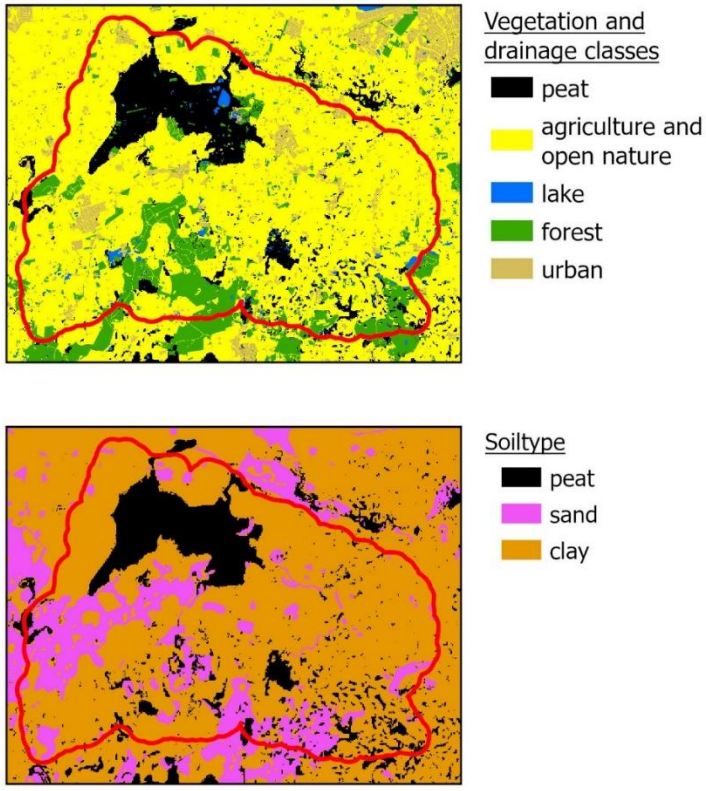

Figure S2: Top: spatial distribution of vegetation and drainage classes in the Tuse catchment model. Class definitions can be seen in Table S1, bottom: Spatial distribution of soil classes in the Tuse catchment model. Class definitions can be seen in Table S2.

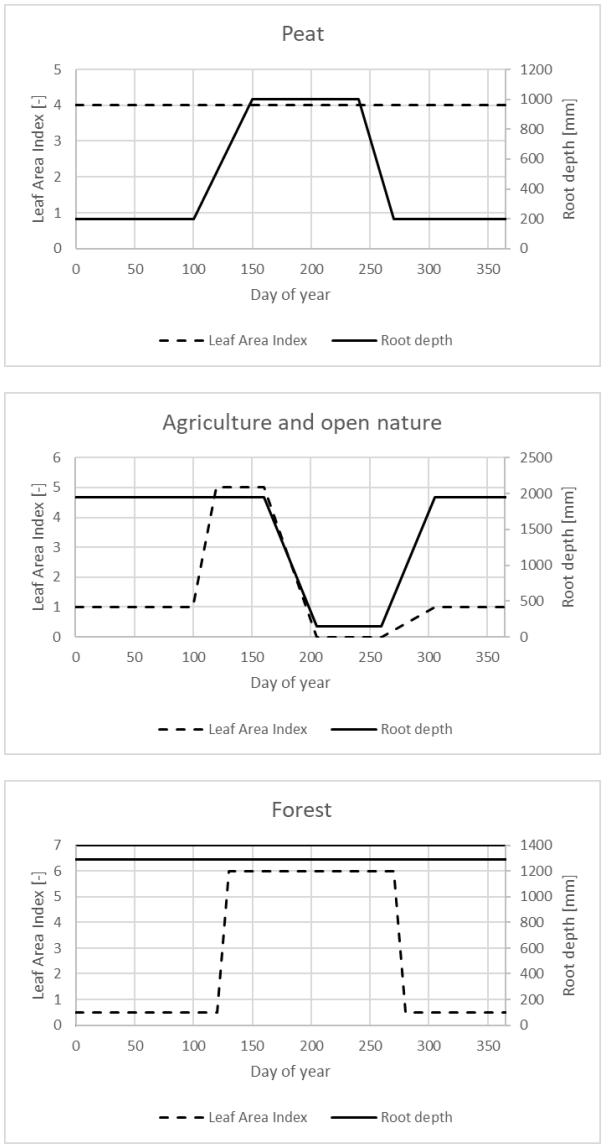

Figure S3: Vegetation development (Leaf Area Index (LAI) and root depth) of peat, agriculture/open nature and forest.

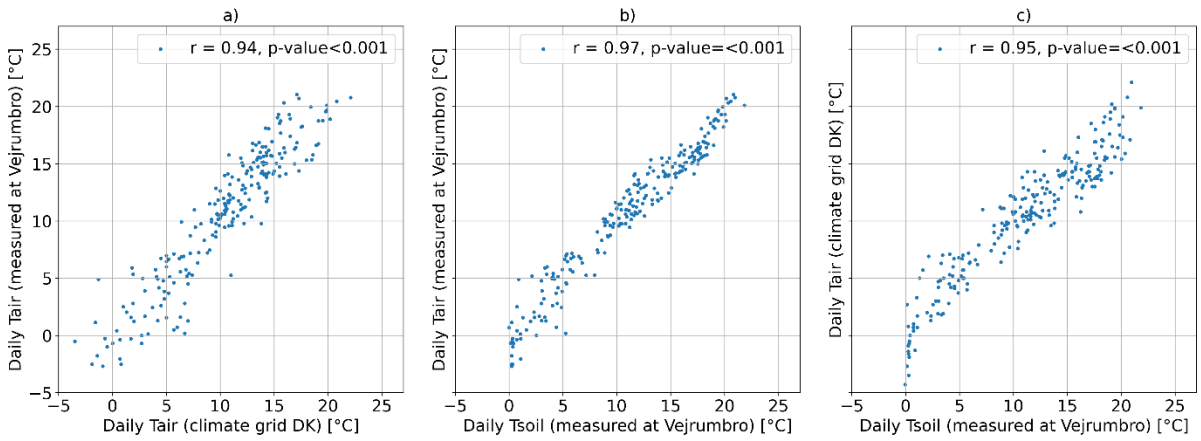

Figure S4: Scatterplots of measured soil temperature at Vejrumbro (Nielsen et al., 2026), measured air temperature at Vejrumbro (Nielsen et al., 2026) and air temperature at Vejrumbro from Climate grid DK (Scharling, 1999a, b).

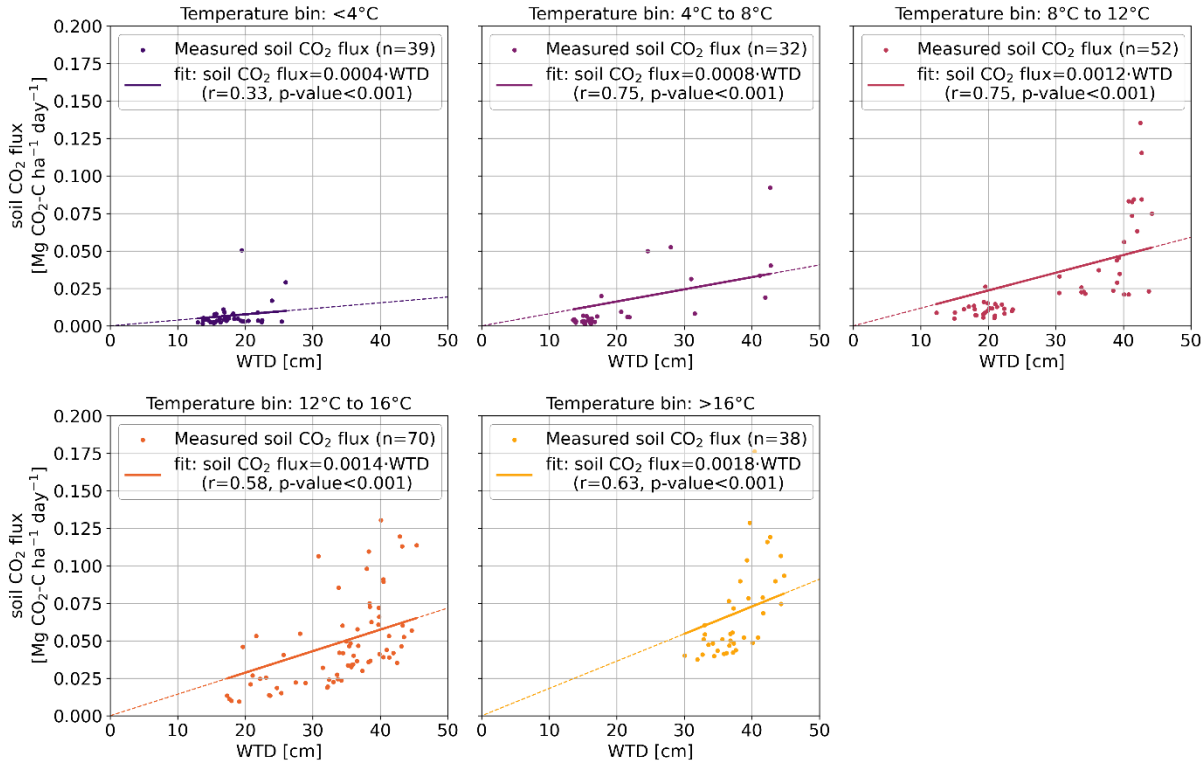

Figure S5: Soil CO_2 flux (R_h) versus WTD (Nielsen et al., 2026) separated in temperature bins.

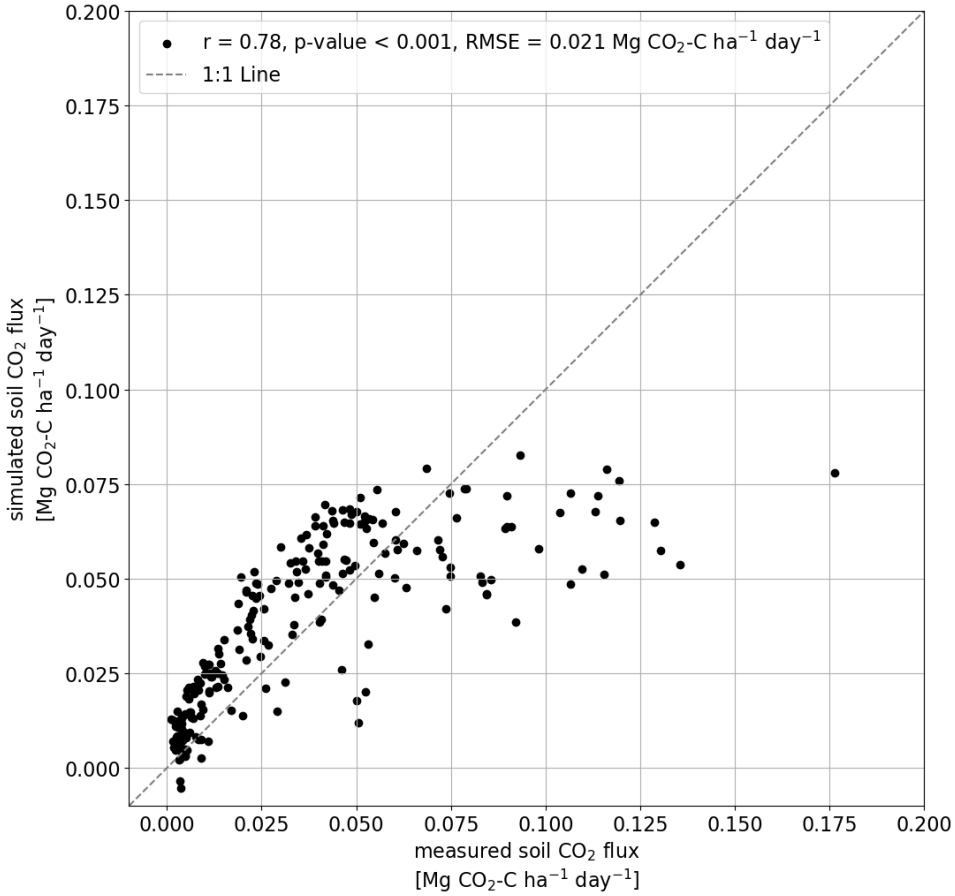

Figure S6: Scatterplot of measured soil CO_2 flux at Vejrumbro (Nielsen et al., 2026) vs. simulated soil CO_2 flux at Vejrumbro with the Daily WTD-T_{air} model. r: Pearsons correlatio coefficient, RMSE: root mean square error.

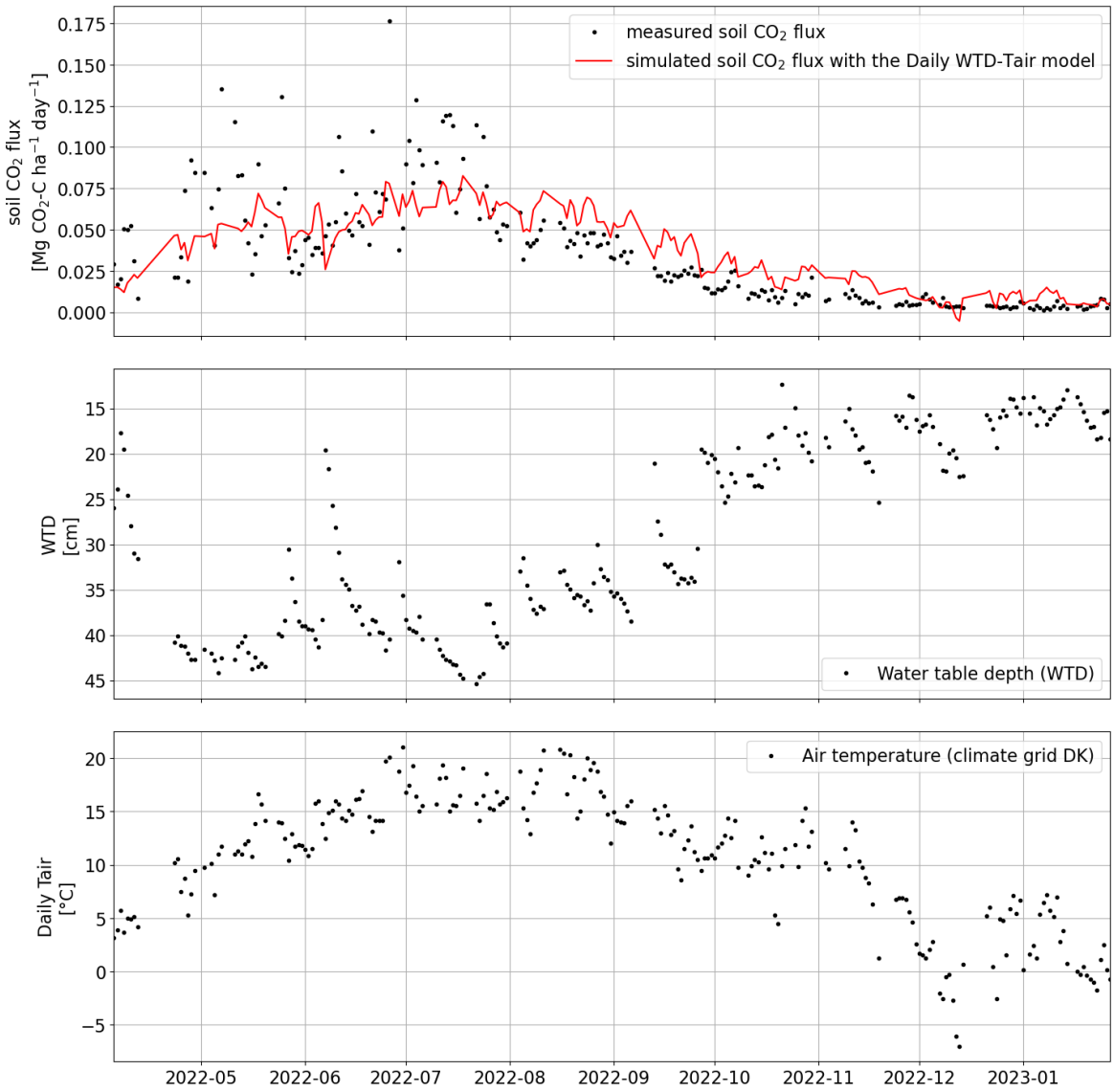

Figure S7: soil CO_2 flux, water table depth (WTD) and air temperature from the Vejrumbro dataset (Nielsen et al., 2026) together with the simulated soil CO_2 flux from the Daily WTD-T_{air} model.

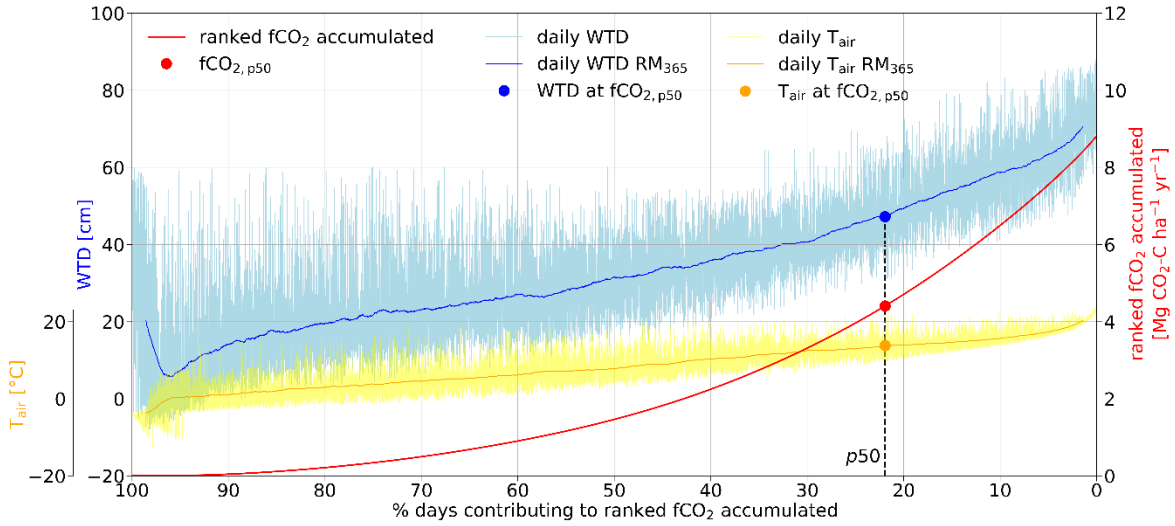

Figure S8: Water table depth (WTD), air temperature (T_{air}) and ranked soil CO_2 flux (fCO_2) accumulated in ascending order based on fCO_2 for the historical simulation period. p50 is the proportion of days required to account for 50% of the total annual fCO_2. RM_{365} is the 365-days running mean.

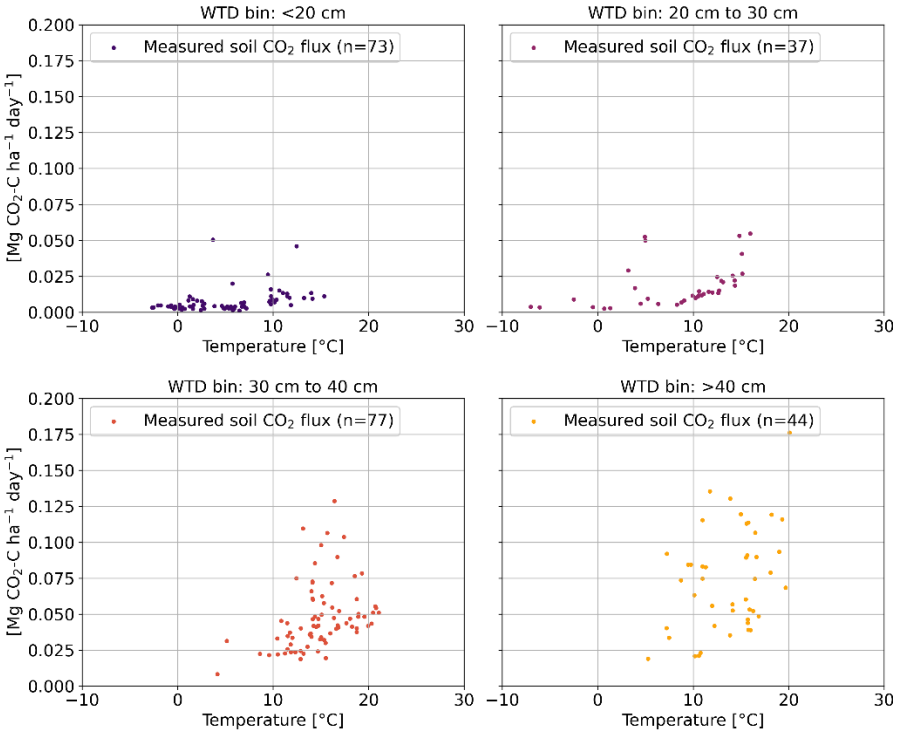

Figure S9: Soil CO_2 flux (R_h) versus temperature (Nielsen et al., 2026) separated in water table depth (WTD) bins.

Table S1: Vegetation and Drain Classes in MIKE SHE Tuse catchment model. The classes are ranked in descending order, meaning that the uppermost layer takes precedence in cases of overlap.

Vegetation/Drain Class in Tuse catchment model	Map of organic Carbon Content (Adhikari et al., 2014)	Landuse BASEMAP (Levin et al., 2017) Landuse classes:
Peat	soil with >6% OC	-
Agriculture and open nature	-	*Agriculture, Nature_open_dry, Nature_open_dry_extensive_agriculture, Nature_open_wet, Nature_open_wet_extensive_agriculture, Road, Rail, Stream, Ressource extraction, Recreation area, Wind energy park, Unclassified*
Lake	-	*Sea, Lake*
Forest	-	*Forest*
Urban	-	*Build-up, City centre, Industry, Airport/runway*

Table S2: Soil classes in MIKE SHE Tuse catchment model. The classes are ranked in descending order, meaning that the uppermost layer takes precedence in cases of overlap.

Soil class in Tuse catchment model	Map of Organic Carbon content (Adhikari et al., 2014)	Danish Digital soil map (Jakobsen et al., 2021) Sedimentation layer (letter symbols):
Peat	soil with >6% OC	-
Sand	-	DG, DS, FS, HG, FG, HS, ZS, MG, MS
Clay	-	FL, FT, FP, SK, ML, DL, SØ, ZG, HL, BY, ZL

Table S3: Water retention parameters (Børgesen et al., 2009), light grey indicates free calibration parameters. Alpha, N, L, Kint are van Genuchten parameters, where Alpha, N and L are empirical constants, and Kint represents the van Genuchtern saturated hydraulic conductivity.

	Unit	Peat	Sand (model soil: 5038)		Clay (model soil: 5077)	
Bulk density	Kg m^{-3}	540	horizon		horizon	
			A	1395	A	1580
			B	1460	B	1700
			C	1660	C	1670
Saturated moisture content	m^3 m^{-3}	0.6	A	0.471	A	0.398
			B	0.447	B	0.421
			C	0.38	C	0.395
Residual moisture content	m^3 m^{-3}	0.06	A	0	A	0
			B	0.003	B	0
			C	0.015	C	0
Alpha	cm^{-1}	0.034	A	0.062	A	0.02
			B	0.059	B	0.041
			C	0.047	C	0.04
N	-	1.312	A	1.306	A	1.205
			B	1.341	B	1.227
			C	1.375	C	1.2
L	-	-2.042	A	-2.137	A	-2.285
			B	-1.583	B	-3.928
			C	-1.196	C	-3.79
Kint	m s^{-1}	$1 \cdot 10^{-9}$	A	$2.84502 \cdot 10^{-6}$	A	$1.98727 \cdot 10^{-7}$
			B	$4.45463 \cdot 10^{-6}$	B	$4.20255 \cdot 10^{-7}$
			C	$1.31134 \cdot 10^{-6}$	C	$3.30903 \cdot 10^{-7}$

Table S4: Hydrological model parameters, light grey indicates free calibration parameters.

		Abbreviation	Unit	Initial parameter value	Lower limit	Upper limit	Log-transformed	Tied to / equation
Evapotranspiration (Vegetation parameters)	Maximum root depth at vegetation class areas of *peat*	RDmax_peat	mm	1000				
	Maximum root depth in vegetation class areas of *agriculture and open nature*	RDmax_agri	mm	1950				
	Maximum root depth in vegetation class areas of *forest*	RD_forest	mm	1290				
	Maximum root depth in vegetation class areas of *urban*	RD_urban	mm	400				
Overland flow	Detention storage	detentionS	mm	15.5936				
Channel flow	Stream-aquifer leakage coefficient	Leak	$m\ s^{-1}$	$1 \cdot 10^{-6}$	$1 \cdot 10^{-7}$	$1 \cdot 10^{-5}$	log10	
Unsaturated zone (Soil parameters)	van Genuchten α at soil class areas of *peat*	Alpha_peat	cm^{-1}	0.034				
	van Genuchten n at soil class areas of *peat*	N_peat	-	1.312				
	Shape factor for hydraulic conductivity at saturation at soil class areas of *peat*	L_peat	-	-2.042				
	Water content in peat soil at saturation at soil class areas of *peat*	ThetaS_peat	-	0.6				
	Factor of residual moisture content at soil class areas of *peat*	ThetaResidual_peat_factor	-	0.5				
	Hydraulic conductivity at saturation at soil class areas of *peat*	Kint	$m\ s^{-1}$	$1 \cdot 10^{-9}$	$1 \cdot 10^{-10}$	$1 \cdot 10^{-6}$	log10	
	Residual moisture content at soil class areas of *peat*	ThetaResidual_peat	-	0.06				ThetaResidual_peat_factor · ThetaS_peat
	Maximum bypass fraction at soil class areas of *peat*	maxBypass_peat	-	0.5	0.25	0.5	-	
	Bypass constant for water content for reduced bypass flow at soil class areas of *peat*	THR1	-	0.3				0.6· maxBypass_peat
	Bypass constant for limit on water content for bypass flow at soil class areas of *peat*	THR2	-	0.1				0.2· maxBypass_peat
Drains	Drain time constant at drainage class areas of *peat*	dt_peat	s^{-1}	$1 \cdot 10^{-8}$	$1 \cdot 10^{-9}$	$1 \cdot 10^{-6}$	log10	
	Drain time constant at drainage class areas of *agriculture and open nature*	dt_agri	s^{-1}	$1 \cdot 10^{-8}$	$1 \cdot 10^{-9}$	$1 \cdot 10^{-6}$	log10	
	Drain time constant at drainage class areas of *forest*	dt_forest	s^{-1}	$1 \cdot 10^{-8}$				dt_agri
	Drain time constant at drainage class areas of *urban*	dt_urban	s^{-1}	$1 \cdot 10^{-8}$				dt_agri
	Drain depth at drainage class areas of *peat*	dd_peat	m	-1.0	-1	-0.2		
	Drain depth at drainage class areas of *agriculture and open nature*	dd_agri	m	-1.0				
	Drain depth at drainage class areas of *forest*	dd_forest	m	-1.0				
	Drain depth at drainage class areas of *urban*	dd_urban	m	-1.0				

Groundwater	Horizontal hydraulic conductivity of 2m top soil, *peat*	Kx_top2m_peat	m s^{-1}	$1 \cdot 10^{-6}$				
	Anisotropy of 2m top soil, *peat*	Aniso	-	10				
	Horizontal hydraulic conductivity of 2m top soil, *clay*	Kx_top2m_clay*	m s^{-1}	$9.75 \cdot 10^{-7}$				
	Horizontal hydraulic conductivity of 2m top soil, *sand*	Kx_top2m_sand*	m s^{-1}	$1.22 \cdot 10^{-3}$				
	Horizontal hydraulic conductivity of sand-layer *kl1*	Kx_kl1*	m s^{-1}	$1.190 \cdot 10^{-7}$	$1 \cdot 10^{-9}$	$5 \cdot 10^{-}6$	log10	
	Horizontal hydraulic conductivity of sand-layer *ks1*	Kx_ks1*	m s^{-1}	$2.438 \cdot 10^{-5}$	$1 \cdot 10^{-}6$	$1 \cdot 10^{-}3$	log10	
	Horizontal hydraulic conductivity of clay-layer *kl2*	Kx_kl2*	m s^{-1}	$1.189 \cdot 10^{-7}$				Kx_kl1
	Horizontal hydraulic conductivity of sand-layer *ks2*	Kx_ks2*	m s^{-1}	$3.181 \cdot 10^{-5}$	$1 \cdot 10^{-6}$	$1 \cdot 10^{-3}$	log10	
	Horizontal hydraulic conductivity of clay-layer *kl3*	Kx_kl3*	m s^{-1}	$1.5 \cdot 10^{-8}$	$1 \cdot 10^{-9}$	$1 \cdot 10^{-6}$	log10	
	Horizontal hydraulic conductivity of sand-layer *ks3*	Kx_ks3*	m s^{-1}	$5.327 \cdot 10^{-5}$	$1 \cdot 10^{-6}$	$1 \cdot 10^{-3}$	log10	
	Vertical hydraulic conductivity of 2m top soil, *peat*	Kz_top2m_peat	m s^{-1}	$1 \cdot 10^{-7}$				$\frac{\text{Kx\_top2m\_peat}}{\text{aniso}}$

*Vertical hydraulic conductivity is a factor 10 lower

Table S5: Climate model projections (Jacob et al., 2014; Pasten-Zapata et al., 2019). Climate model projection no. 5 was used as forcing data for the Tuse catchment model in Figure 8 of the main manuscript.

No.	Climate model projections	Periode
1	CCCma-CanESM2_rcp85_r1i1p1_GERICS-REMO2015_v1	1971-2100
2	CNRM-CERFACS-CNRM-CM5_rcp85_r1i1p1_CLMcom-CCLM4-8-17_v1	1971-2100
3	ICHEC-EC-EARTH_rcp85_r1i1p1_KNMI-RACMO22E_v1	1971-2100
4	ICHEC-EC-EARTH_rcp85_r3i1p1_DMI-HIRHAM5_v1	1971-2100
5	**ICHEC-EC-EARTH_rcp85_r12i1p1_KNMI-RACMO22E_v1**	**1971-2100**
6	IPSL-IPSL-CM5A-MR_rcp85_r1i1p1_SMHI-RCA4_v1	1971-2100
7	MIROC-MIROC5_rcp85_r1i1p1_GERICS-REMO2015_v1	1971-2100
8	MOHC-HadGEM2-ES_rcp85_r1i1p1_CLMcom-CCLM4-8-17_v1	1971-2099
9	MOHC-HadGEM2-ES_rcp85_r1i1p1_DMI-HIRHAM5_v1	1971-2099
10	MOHC-HadGEM2-ES_rcp85_r1i1p1_GERICS-REMO2015_v1	1971-2099
11	MOHC-HadGEM2-ES_rcp85_r1i1p1_KNMI-RACMO22E_v2	1971-2099
12	MOHC-HadGEM2-ES_rcp85_r1i1p1_SMHI-RCA4_v1	1971-2099
13	MPI-M-MPI-ESM-LR_rcp85_r1i1p1_MPI-CSC-REMO2009_v1	1971-2100
14	MPI-M-MPI-ESM-LR_rcp85_r1i1p1_SMHI-RCA4_v1a	1971-2100
15	MPI-M-MPI-ESM-LR_rcp85_r2i1p1_MPI-CSC-REMO2009_v1	1971-2100
16	NCC-NorESM1-M_rcp85_r1i1p1_DMI-HIRHAM5_v2	1971-2100
17	ICHEC-EC-EARTH_rcp85_r12i1p1_SMHI-RCA4_v1	1971-2100

Table S6: Analysis of spatial variability. Pearsons's correlation coefficient r between a number of spatial variables and observed and simulated annual mean water table depth (ME_{WTD}).

			Correlation coefficient r	
spatial variable	Source	No. of observation wells	observed mean annual WTD ME_{WTD}	simulated mean annual ME_{WTD}
Observed thickness of peat layer	This paper	13	-0.34	0.27
TWI (20m grid)	(Klimadatastyrelsen, 2025)	22	-0.21	0.21
Terrain slope (20m grid)	(Klimadatastyrelsen, 2025)	22	0.10	0.01
Horizontal distance to drain ditches	(Klimadatastyrelsen, 2025)	22	0.09	-0.25
Horizontal distance to nearest river/ lake	(Klimadatastyrelsen, 2025)	22	0.11	-0.18
Vertical distance to drain ditches	(Klimadatastyrelsen, 2025)	22	-0.20	0.20
Vertical distance to river/lake	(Klimadatastyrelsen, 2025)	22	-0.18	0.19
Cropping history – rankede wetness	(Koch et al., 2023)	22	-0.18	0.17

Table S7: Model performance and variable correlation. Coefficient of determination (R^2) between soil CO_2 flux observed at Vejrumbro and soil CO_2 flux simulated with Daily WTD-T_{air} model and three empirical CO_2 emission models from (Rigney et al., 2018) (fitted to observed CO_2 flux at Vejrumbro), respectively, as well R^2 between the modelled soil CO_2 flux and input variables T_{air} and WTD. [6], [7] and [8] refer to the equation number in (Rigney et al., 2018).

	Equation	R^2_{Obs} (simulated CO_2 vs observed CO_2)	R^2_{Tair} (simulated CO_2 vs T_{air})	R^2_{WTD} (simulated CO_2 vs WTD)
Daily WTD-T_{air} model	$b \cdot T_{air} \cdot WTD + c \cdot WTD$	0.61	0.34	0.54
[6]	$a \cdot \exp\left(b \cdot \left(\frac{1}{T_{ref} - T_0} - \frac{1}{T_{air} - T_0}\right)\right) + (WTD \cdot c)^2$	0.62	~0	0.94
[7]	$a + (b \cdot WTD) \cdot \exp\left(c \cdot \left(\frac{1}{T_{ref} - T_0} - \frac{1}{T_{air} - T_0}\right)\right)$	0.62	0.10	0.86
[8]	$a \cdot \exp\left(c \cdot \left(\frac{1}{T_{ref} - T_0} - \frac{1}{T_{air} - T_0}\right)\right) + b \cdot WTD$	0.61	~0	~1

References

Adhikari, K., Hartemink, A. E., Minasny, B., Bou Kheir, R., Greve, M. B., and Greve, M. H.: Digital mapping of soil organic carbon contents and stocks in Denmark, PLoS One, 9, https://doi.org/10.1371/journal.pone.0105519, 2014.

Børgesen, C. D., Waage-Petersen, J., Iversen, T. M., Grant, R., Jacobsen, B., and Elmhold, S.: Midtvejsevaluering af vandmiljøplan III – Hoved og baggrundsnotater, Det Jordbrugsvidenskabelige Fakultet, Århus Universitet, DJF rapport markbrug 142, 2009. ISBN 87-91949-44-0

Jacob, D., Petersen, J., Eggert, B., Alias, A., Christensen, O. B., Bouwer, L. M., Braun, A., Colette, A., Déqué, M., Georgievski, G., Georgopoulou, E., Gobiet, A., Menut, L., Nikulin, G., Haensler, A., Hempelmann, N., Jones, C., Keuler, K., Kovats, S., Kröner, N., Kotlarski, S., Kriegsmann, A., Martin, E., van Meijgaard, E., Moseley, C., Pfeifer, S., Preuschmann, S., Radermacher, C., Radtke, K., Rechid, D., Rounsevell, M., Samuelsson, P., Somot, S., Soussana, J. F., Teichmann, C., Valentini, R., Vautard, R., Weber, B., and Yiou, P.: EURO-CORDEX: New high-resolution climate change projections for European impact research, Reg Environ Change, 14, 563–578, https://doi.org/10.1007/s10113-013-0499-2, 2014.

Jakobsen, P. R., Tougaard, L., and Anthonsen, K. L.: Danmarks Digitale Jordartskort 1:25.000, version 5.0, GEUS, 2021.

Klimadatastyrelsen: Danmarks Højdemodel, Danish Elevation model (DK-DEM), Danish Agency for Data Supply and Infrastructure, Retrieved from https://dataforsyningen.dk, 2025.

Koch, J., Elsgaard, L., Greve, M. H., Gyldenkærne, S., Hermansen, C., Levin, G., Wu, S., and Stisen, S.: Water-table-driven greenhouse gas emission estimates guide peatland restoration at national scale, Biogeosciences, 20, 2387–2403, https://doi.org/https://doi.org/10.5194/bg-20-2387-2023, 2023.

Kristensen, K. J. and Jensen, S. E.: A model for estimating actual evapotranspiration from potential evapotranspiration, Nordic Hydrology, 170–188, 1975.

Levin, G., Iosub, C.-I., and Jepsen, M. R.: Basemap02, Technical documentation of a model for elaboration of a land-use and land-cover map for Denmark, 64 pp., 2017.

Nielsen, A. S., Larsen, K. S., Lærke, P. E., Rodriguez, A. F., Pullens, J.W. M., Petersen, R. J., and Christiansen, J. R.: A full year of continuous net soil and ditch CO2, CH4, N2O fluxes, soil hydrology and meteorology for a drained fen in Denmark, Earth Syst. Sci. Data, 18, 33–53, https://doi.org/10.5194/essd-18-33-2026, 2026.

Pasten-Zapata, E., Sonnenborg, T. O., and Refsgaard, J. C.: Climate change: Sources of uncertainty in precipitation and temperature projections for Denmark, Geological Survey of Denmark and Greenland Bulletin, 43, 1–6, https://doi.org/10.34194/GEUSB-201943-01-02, 2019.

Rigney, C., Wilson, D., Renou-Wilson, F., Müller, C., Moser, G., and Byrne, K. A.: Greenhouse gas emissions from two rewetted peatlands previously managed for forestry, Mires and Peat, 21, 1–23, https://doi.org/10.19189/MaP.2017.OMB.314, 2018.

Scharling, M.: Klimagrid Danmark - Nedbør, lufttemperatur og potentiel fordampning 20X20 & 40x40 km - Metodebeskrivelse, Danish Meteorological Institute, ISSN-nr.0906-897X, ISSN-nr.1399-1388 (online), 1999a.

Scharling, M.: Klimagrid Danmark Nedbør 10x10 km (ver. 2) - Metodebeskrivelse, Danish Meteorological Institute, ISSN-nr.0906-897X, ISSN-nr.1399-1388 (online), 1999b.